Speed-Spacing Dependency on Relative Speed from the Adjacent Lane: New Insights for Car Following Models

Manuscript TRB-D-15-00283

Balaji Ponnu

Graduate Research Assistant
The Ohio State University
Department of Civil, Environmental, and Geodetic Engineering

Benjamin Coifman, PhD

Associate Professor
The Ohio State University
Joint appointment with the Department of Civil, Environmental, and Geodetic Engineering, and the Department of Electrical and Computer Engineering

Hitchcock Hall 470
2070 Neil Ave, Columbus, OH 43210
Phone: (614) 292-4282
E-mail: Coifman.1@OSU.edu

Abstract

This paper examines the traffic dynamics underlying a recently observed phenomenon, the so called "sympathy of speeds" whereby a high occupancy vehicle (HOV) lane seemingly exhibits lower vehicular capacity and lower flow at speeds throughout the congested regime compared to the adjacent general purpose (GP) lanes. Unlike previous studies this paper examines a time-of-day HOV lane. During the non-HOV periods the study lane reverts to a GP lane, thereby providing a control condition for the specific lane and location. This work uses the single vehicle passage (svp) method to group vehicle passages before measuring the traffic state and extends the svp to bin vehicles in the study lane based on the relative speed to the adjacent lane. The extended svp method allows the work to also study the impacts during the non-HOV periods when the study lane serves GP vehicles. This work finds that: (1) During the non-HOV periods the study lane exhibited behavior indistinguishable from the adjacent GP lane. (2) The sympathy of speeds persists throughout the day, even when the study lane serves GP vehicles. (3) The relative speed to the adjacent lane provided a better predictor of behavior than whether or not the HOV restriction is active. In short, the car following behavior that gives rise to the sympathy of speeds is unrelated to the HOV restriction per se, persisting under GP operations as well.

This dependency on the relative speed in the adjacent lane is an important finding given the fact that most existing car following models assume that the longitudinal acceleration of a following vehicle is strictly a function of the relationship to the leading vehicle in the same lane. Because drivers in general adopt a larger spacing when faced with a high differential in speed between lanes means that car following behavior also depends on the relative speed to the adjacent lane. This fact has likely gone unnoticed to date because generally the conditions that give rise to a differential in speeds between lanes are usually short lived, and thus, do not become apparent in conventional macroscopic data except under exceptional circumstances that include confounding factors like HOV operations.

Keywords

Traffic flow theory, car following, fundamental relationship, speed-spacing relationship, loop detectors, highway traffic, microscopic models, HOV operations

Highlights

- HOV lanes exhibit lower flow at speeds throughout the congested regime
- Results show that this difference is not due to HOV operations per se
- The difference arises from relative speed between lanes, even for GP drivers
- Drivers adopt larger spacing when faced with high relative speed between lanes
- This dependence on adjacent lanes is absent from most car following models

1. Introduction

A few traffic operations studies have observed that high occupancy vehicle (HOV) lanes exhibit markedly different dynamics than the adjacent general purpose (GP) lanes. They found that compared to the GP lanes, the HOV lanes typically have a lower vehicular capacity[1] and more recently it has been found that this trend continues into the congested regime whereby the HOV lanes exhibit a lower flow at a given occupancy, occ, or density, k, during congestion, e.g., as shown in Fig. 1a-b with lane 1 and lane 2 respectively being adjacent HOV and GP lanes. While the prior studies have observed this *sympathy of speeds* macroscopically in the context of traffic operations, e.g., whether HOV lanes reduce net vehicular capacity, there has been little attention paid to the underlying traffic dynamics in the context traffic flow theory. To this end the current work seeks to uncover the microscopic behavior that gives rise to the emergent macroscopic relationships studied previously.

Unlike the previous studies this work examines a time-of-day, continuous-access HOV lane. During the non-HOV periods the study lane reverts to a GP lane, thereby providing a control condition for the specific lane and location. Furthermore, to avoid potentially mixed traffic conditions that simultaneously exhibit behaviors from both the free flow and congested regimes the focus of this study is primarily congested flows below the apparent vehicular capacity. This work uses the single vehicle passage (svp) method to calculate the flow-occupancy fundamental relationship, qoccFR. As discussed in greater detail below, the svp sorts individual vehicle measurements into separate bins based on length and speed before measuring flow, q, and occupancy individually for each bin. The svp method gives rise to very clean qoccFR that do not require stationary traffic or any prior assumption of the underlying shape of the curve. With homogeneous vehicle lengths in each bin, occupancy can be cleanly projected to density, yielding the macroscopic flow-density fundamental relationship, qkFR. This study extends the svp method by adding a third dimension to the binning process, so vehicles are now also sorted by relative speed to the adjacent lane. In the analysis this work makes several insights: First, by using the time-of-day HOV lane the study finds that during the non-HOV hours the inactive HOV lane exhibits qkFR similar to the GP lane throughout the congested regime. Thereby providing a control condition to compare the active HOV qkFR against. Second, this work further exploits the homogeneous vehicle lengths in the svp bins by projecting the macroscopic qkFR to the microscopic speed-spacing relationship, VXp, so that the results can be cleanly interpreted in terms of car following behavior. Third, because the svp method takes vehicles individually, the homogeneity extends to each dimension of the binning process. So even when the HOV restriction is inactive and the study lane is serving GP vehicles the extended svp method preserves the dimensional influence of the given factor on the individual drivers, thus, all vehicles in a given bin have the same relative speed to the adjacent lane.

[1] Where the vehicular capacity is the vehicular flow at the apex of the flow-occupancy curve. Furthermore, when speaking of HOV facilities it is necessary to distinguish between person flow and vehicular flow. Since the focus of this work is traffic dynamics, this paper only considers vehicular flow and capacity. Given the need for a clear person versus vehicular distinction, the authors use *vehicular capacity* instead of their preferred terminology, *roadway capacity*, to refer to the vehicular flow at the apex of the flow-occupancy curve at a given location along the roadway. Throughout this paper "capacity" or "vehicular capacity" refer to the roadway capacity. In general there is also a need to distinguish between roadway capacity at a given location along the road from the potentially unrelated *bottleneck capacity* that gives rise to queue formation and limits the vehicular flow through the entire corridor. Since the study location is far upstream of any recurring bottlenecks the bottleneck capacity is not considered in this work.

As will be shown, the sympathy of speeds arises because a large differential in speed between lanes causes the faster drivers to be more conservative on average and take larger spacing at a given speed (or a lower speed at a given spacing). While this outcome is consistent with the previous operational studies of HOV facilities, most of those studies erroneously attributed it specifically to the HOV operation. By taking care to preserve the influence of the relative speed to the adjacent lane during the non-HOV period this work shows that the dependency on the adjacent lane persists during the GP operations. In other words the car following behavior that gives rise to the sympathy of speeds is unrelated to the HOV restriction per se, since the sympathy of speeds is also observed under GP operations.

This last finding is important since most existing car following models assume that the longitudinal acceleration of a following vehicle is strictly a function of speed and spacing to the leading vehicle in the same lane. Because drivers in general adopt a larger spacing when faced with a high differential in speed between lanes means that actual car following behavior also depends on the relative speed to the adjacent lane. This fact has likely gone unnoticed in GP lanes to date because generally the conditions that give rise to a differential in speeds between lanes are usually short lived, and thus, do not become apparent in conventional macroscopic data that arbitrarily group inhomogeneous vehicles together based on arrival order. In such sequential grouping the influence from a sympathy of speeds is obscured due to rapidly changing conditions except under exceptional circumstances that include confounding factors like HOV operations where the differential in speed arising from the priority vehicles can be sustained for extended time periods.

1.1. Overview

Section 2 provides background necessary to place this work in context. Section 3 presents the empirical data used in this work, reproduces past observations of HOV operations, and then dissects the findings in the context of traffic flow theory. This section ultimately reveals that the phenomena arises due to relative speed and it is also observed when the study lane is serving GP vehicles during the non-HOV period. This paper closes with a discussion and conclusions in Section 4.

2. Background

This section reviews the prior research related to the traffic dynamics as well as the tools used for the present work. Section 2.1 reviews the literature on HOV operations, Section 2.2 reviews the relevant traffic flow theory on car following, and Section 2.3 introduces the svp method that forms the basis of the analysis in the remainder of this paper.

2.1. HOV Operations

In the freeway operations literature it has been known for some time that HOV lanes exhibit lower vehicular capacity than GP lanes (e.g., Xu et al., 1999). Martin et al. (2002) studied a limited-access HOV lane separated from the GP lanes by double solid stripes and observed a *sympathy of speeds* whereby, "the HOV lanes do not operate at expected speeds relative to the volume. For example, the speeds of an HOV lane, adjacent to a congested GP lane, are often less than the speed limit even though the flow is well below capacity." They attributed this sympathy of speeds to the fact that an HOV driver is uncomfortable with a large disparity in speed between their lane and the adjacent, congested GP lane. Guin et al. (2008) studied a continuous-access

HOV lane separated from the GP lanes by dashed stripes and also found a sympathy of speeds in the HOV lane due to congestion on the adjacent GP lane. Manda et al. (2011) found the vehicular capacity of barrier-separated HOV facilities to be 10%-30% lower than the adjacent GP lanes and Liu et al. (2011, 2012) found that the sympathy of speeds also occurs in barrier-separated HOV lanes. While these studies observed a lower vehicular capacity in the HOV lane and a few also observed that the lower flows extended into the congested regime, they were focused by and large on simply showing that the HOV lane exhibits a single, static fundamental relationship that is different from the GP lanes.

Two studies went further and showed evidence that the fundamental relationship in the HOV lane actually depends on conditions in the adjacent GP lane. First, Thomson et al. (2012) examined two types of HOV facilities: continuous access and limited access with buffer zone. To account for the *friction* arising from the adjacent GP lane they derived two separate speed-flow curves (vqFR curves) for the given HOV lane. When the GP lane was below 35 pcpmpl the HOV vqFR relationship was assumed to follow one vqFR curve and when the GP lane was above 35 pcpmpl the HOV vqFR relationship was assumed to follow a lower vqFR curve (i.e., q(v) was lower in the second condition). Second, Jang et al. (2012) studied the qkFR for both continuous-access HOV lanes separated from the GP lanes by dashed stripes and limited-access HOV lanes separated from the GP lanes by double solid stripes and a buffer zone. Rather than assuming simply two static curves as was done by Thomson et al., Jang et al. sorted the HOV measurements as a function of 10 mph speed bins in the adjacent GP lane. While both types of HOV lanes exhibited lower vehicular capacity than the adjacent GP lanes, Jang et al. found an explicit dependency of HOV speeds on the adjacent GP lane speeds for the continuous-access HOV lanes and no apparent speed dependency for the buffer-separated limited-access HOV lanes.

Both Thomson et al. and Jang et al. focused on operations, e.g., developing guidelines for the Highway Capacity Manual. The studies were strictly macroscopic and presumed that the relationships were simply characteristic of HOV facilities. While these works are beneficial for operations, neither paper pursued the implications in the context of traffic flow theory or driver behavior. Both papers misinterpreted maximum observed HOV throughput at a given GP state as being the capacity of the HOV lane, failing to recognize the fact that a given lane might not exhibit its vehicular capacity if constrained by other factors (see, e.g., Coifman and Kim, 2011; Kim and Coifman, 2013). Furthermore, both papers estimated density without correctly accounting for an inhomogeneous vehicle fleet (see, e.g., Coifman, 2015).

Finally, Jang and Cassidy (2012) used a special opportunity arising from a regulatory change to effectively examine the speed-flow relations on HOV lanes. California had allowed single occupant Low-Emitting Vehicles (LEVs) to travel in HOV lanes until the state reversed the policy and prohibited this practice in 2011. The authors found that when these LEVs are forced out of HOV lanes that the HOV lane experiences lower speeds even though the lane's flow is also reduced. They attributed the drop in HOV lane speeds to the dependency of the HOV lane on the adjacent GP lane's speed, which in turn dropped in response to the added LEVs.

2.2. Car Following Models

Moving from the operations perspective in Section 2.1 to traffic flow theory, presumably HOV driver behavior is independent of the fact that the traffic conditions arise from an active HOV restriction, and instead the HOV drivers continue to exhibit the same car following behavior that they also exhibit on GP lanes. Reviewing the literature, most car following models

only consider the following vehicle's response to the immediate leading vehicle in the same lane and assume that the car following is not interrupted by lane change maneuvers. These models typically express the following vehicle's longitudinal acceleration as a function of one or more independent variables, with the most common being the speed of the follower, relative speed between the two vehicles, and relative spacing between the two vehicles. Examples of such models are the *General Motors Models* (Chandler et al., 1958; Gazis et al. 1959; Herman and Potts, 1959; Gazis et al., 1961), *Collision Avoidance Models* (Kometani and Sasaki, 1958; Gipps, 1981), *Psycho-Physical Models* (Montroll, 1959; Michaels, 1963; Lee and Jones, 1967; Evans and Rothery, 1973, 1977; Lee, 1976; Leutzbach and Wiedemann, 1986; Reiter, 1994; Kumamoto et al., 1995; Fellendorf and Hoyer, 1997, Sauer, 2003; Jin et al., 2011a), the *Optimal Velocity Model* (Bando et al., 1995), and the *Intelligent Driver Model* (Treiber et al, 2000).

In pursuit of more stable car following behavior, several recent models in the physics community have adopted a multi-vehicle look-ahead, whereby the following vehicle effectively responds to several leading vehicles in the follower's lane of travel (e.g., Lenz et al., 1999; Nagatani, 1999; Ge et al., 2004; Wilson et al., 2004; Liu et al., 2008; Peng and Sun, 2010). There is also a growing body of combined car following and lane change maneuver models where the follower considers several leaders (e.g., Treiber and Kesting, 2009; Luo and Boloni, 2012). In this case, the following driver not only considers their same lane leader for car following, but they also consider the adjacent lane vehicles in the context of initiating and executing lane change maneuvers. However, the consideration of the adjacent lane(s) is only in the context of lane change maneuvers, aside from contemplating or executing lane change maneuvers the car following behavior remains strictly a function of vehicles in the follower's lane of travel.

Only a few car following models explicitly contemplate the possibility that the adjacent lane directly influences car following behavior away from lane change maneuvers. Tang et al. (2005) extended the optimal velocity model to include a factor to also account for the distance to the leading vehicle in the adjacent lane. They developed the model in the context of Beijing traffic where the authors observed that some drivers would abruptly change lanes without notice, and so the authors conjectured that in general drivers would behave cautiously to the lead vehicle in an adjacent lane in case that neighboring vehicle would suddenly enter their own lane. Jin et al. (2010) also modified the optimal velocity model, in this case to include multiple leaders to account for staggered arrangement of cars on the roadway due to a lack of lane-discipline on Chinese roads and found that the model yielded more stable results; however, their model reverts back to a single leader in the follower's lane as soon as any other potential leader is completely in an adjacent lane.

Gunay (2007) extended Gipps' model to include lateral effects between lanes. The study was motivated by empirical evidence that drivers often slow down as they overtake another vehicle in an adjacent lane. The simulated results exhibited similar relationships to an empirical study of an overtaking vehicle's speed relative to the lateral distance to the overtaken vehicle. Jin et al. (2011b) extended Gazis et al. (1961) to form a non-lane based car following model in which a driver might respond neighboring vehicles in addition to the same lane leader, depending on the lateral separation to the neighboring vehicles. One result is that like Gunay, a vehicle may slow down while overtaking a vehicle in an adjacent lane. Jin et al. (2012) repeats this exercise only now based upon the optimal velocity model. With the exception of Gunay, these car following models that include the influence of the adjacent lane were evaluated strictly based on simulation results, without any empirical validation or calibration. While the general

forms of these models are promising, they have yet to enter common practice and the need remains for empirical study.

2.3. The Single Vehicle Passage Method

While the roots of the sympathy of speeds studied in the current work were first observed in the traffic operations literature (Section 2.1) and the ultimate goal is to empirically associate the phenomena with car following behavior (Section 2.2), the process of making that connection will use the single vehicle passage method (svp). The svp method was developed in the context of the flow-occupancy relationship, qoccFR, by Coifman (2014b) as applied to dual loop detector data and summarized as follows. In the svp methodology vehicles are no longer taken successively in the order in which they arrived and there is no requirement to seek out stationary traffic conditions; rather, for each and every individual vehicle passage the traffic state is measured over the headway, h (thus, by definition, avoiding partial headways) and the vehicles are grouped by similar lengths (thus, avoiding an inhomogeneous fleet) and then grouped by speed before aggregation. Flow, q_{svp}, for each individual svp is calculated via Equation 1. The associated detector on_time is measured and is used in conjunction with h to calculate the occupancy, occ_{svp}, via Equation 2 (note that h is measured *rear bumper to rear bumper* to ensure that the gap ahead of a vehicle is associated with its own on_time). The corresponding speed, v_{svp}, and vehicle length, L_{svp}, are then calculated via Equations 3-4 following conventional methods.

$$q_{svp} = \frac{1}{h} \tag{1}$$

$$occ_{svp} = \frac{on\_time}{h} * 100\% \tag{2}$$

$$v_{svp} = \frac{detector\_spacing}{traversal\_time} \tag{3}$$

$$L_{svp} = v_{svp} * on\_time \tag{4}$$

The vehicles are sorted into L_{svp} bins that only span 5 ft or 10 ft. The vehicles in each length bin are then treated separately from the other length bins. Within a given length bin the vehicles are further sorted into v_{svp} bins that only span 1 mph. The result is a homogeneous set of vehicles and speeds in each length-speed bin without regard for the presence or absence of stationary traffic conditions. To ensure the largest possible number of similar vehicles per sample, the median q_{svp} and median occ_{svp} are found for each combined length and speed bin. Only bins containing at least 100 observations were retained (thus, ensuring a large sample size). Like Coifman (2014b), throughout the current work any bin with fewer than 100 samples is not shown.

Coifman (2015) extends the svp to measure the macroscopic flow-density relationship, qkFR, and the corresponding microscopic speed-spacing relationship, VXp, from dual loop detector data. Key to this extension is the fact that the svp method sorts vehicles by length at the start, so the final qoccFR curves for a given length bin arise from homogeneous vehicles. Or flipping this logic around, the small range of vehicle lengths in a given qoccFR curve from the svp method gives rise to special properties; in particular, the homogeneous length range in each svp length bin allows for direct application of Equation 5 to derive density, k_{svp}, where L_{eff} is the median L_{svp} in the given bin. This conversion is something that cannot be done (correctly) with conventional fixed time measurements from inhomogeneous vehicles. By extension the average spacing, $\bar{x}_{svp}$, for each bin comes from the reciprocal of k_{svp} via Equation 6, yielding the

microscopic VXp. Coifman (2015) also verified the resulting dual loop detector based VXp against VXp from microscopic vehicle trajectory data. Fig. 1 shows an example of qoccFR from dual loop detector data, along with the corresponding qkFR and VXp.

$$k_{svp} = \frac{occ_{svp}}{L_{eff}} \tag{5}$$

$$\bar{x}_{svp} = \frac{1}{k_{svp}} \tag{6}$$

Of course taking the median spacing within a bin via Equation 6 (or median occupancy via Equation 2) should only perform well in the congested regime, where most drivers will be car following. At higher speeds, many drivers will reach their desired free speed and then choose a large spacing that does not depend on speed. At which point, the performance of the svp method binning by speed should degrade (Coifman, 2015). Fortunately, this work focuses on the congested regime, where the free flow behavior has little impact.

Overall the use of the svp method brings robustness to the analysis. The preceding macroscopic traffic flow studies reviewed in Section 2.1 all relied on detector data conventionally aggregated over successive fixed time sampling periods. Coifman and Wang (2005) showed that conventionally measured flow and occupancy are functions of the underlying vehicle lengths, while Coifman (2001) found that the distribution of vehicle lengths varies both as a function of the time-of-day and as a function of the traffic conditions (e.g., trucks may actively seek to avoid congested conditions). It is impossible to separate trends in conventionally measured flow and occupancy from the unobserved vehicle lengths. Coifman (2014a) went into greater depth analyzing the length dependence and explored many sampling errors that impact measurements from conventional fixed time sampling periods. These factors degrade conventionally aggregated detector data and were the motivation for developing the svp method (Coifman 2014b) and the svp method has been shown to be far more robust to these factors (Coifman 2014b, 2015).

3. Analysis

The analysis begins with Section 3.1 presenting the empirical data used in this work. Section 3.2 uses these data to examine the HOV behavior and dissects the findings in the context of traffic flow theory. Then Section 3.3 fits regression models to the empirical data.

3.1. Data Description

This work examines traffic in a time-of-day, continuous-access HOV lane and the immediately adjacent GP lane. The data come from the two innermost lanes, lanes 1-2, out of a total of five lanes at eastbound stations 1-4 and 6 in the Berkeley Highway Laboratory (Coifman et al., 2000) along a roughly two mile stretch of I-80, just north of Oakland, CA[2]. The two study lanes were separated with conventional dashed striping used between GP lanes. The only distinction between the two lanes was the time-of-day signage and the diamond pavement markings in the HOV lane. This work uses individual svp data from all five stations observed on 69 weekdays between September 1 and December 31, 1999. The remaining 19 weekdays in this window of dates were excluded for one or more of the following three reasons: no observed

[2] Station 5 was excluded because one loop detector in lane 1 was inoperable, thus, preventing speed measurement. Meanwhile, as of publication the data set is available at http://www.ece.osu.edu/~coifman/documents/

congestion on that day, a holiday, or suspect time stamps due to incorrectly accounting for the end of Daylight Savings Time.

The top row of Table 1 reports the total number of svp measurements by lane from the 69 days. As evident in the table, this work will usually refer to the two lanes by their lane number, with lane 1 being the time-of-day HOV lane and lane 2 being the strictly GP lane. Since some of the conditions of interest in this study are relatively uncommon, to achieve sufficient sample size the current study combines the data across all of the days and all of the stations before calculating the median q_{svp} and median occ_{svp} for each bin under a given condition (e.g., during the HOV period). Furthermore, comparing the top two rows of Table 1, passenger vehicles (defined to be L_{svp} falling between 18 and 22 ft) make up over 70% of the vehicles observed in either lane. This fact arises for several reasons- passenger vehicles typically make up the majority of the vehicles on urban freeways and at this specific location trucks are prohibited in lanes 1 and 2.[3] As a result, to ensure sufficient sample size in the binned data this work only examines the passenger vehicles.

The HOV restriction is active 5:00-10:00 and 15:00-19:00, with lane 1 reverting to a GP lane outside of these periods. The dominant flow in the morning peak is westbound and so the eastbound lanes used in this study see very little congestion during the morning HOV window. In the evening the eastbound lanes see heavy demand and most weekdays exhibit congestion in this corridor.

As such, the vehicles are further delineated by time periods. This work uses the HOV hours of 15:00-19:00 as the *HOV period* for the stations under study, while the *non-HOV period* is set to the combined hours of 13:00-14:45 and 19:15-21:00. This selection provides a 15 min buffer before and after the HOV period to allow drivers to adjust for the start/end of the HOV restriction, captures most of the recurring congestion that falls outside of the HOV period, and avoids atypical traffic conditions that can arise at night, e.g., a higher percentage of trucks (Coifman, 2001). The final data used in this study come from these time-of-day periods across all 69 days, across all five stations.[4] Table 1 tallies the total number of vehicles seen in these conditions by lane as well as the number with speeds below 40 mph, 50 mph and 65 mph for the HOV and non-HOV periods. With the focus on congested conditions, on most days the effective non-HOV period with speeds of interest is a lot shorter, starting much later than 13:00 and ending much earlier than 21:00.

3.2. Application

If for the moment one naively combines all of the data from all 24 hrs of the day together for a given lane, Fig. 1a shows the resulting qoccFR by lane after applying Equations 1-4 to the data from Section 3.1, sorting out the passenger vehicles (18-22 ft), binning these by 1 mph bins, then finding the median q_{svp} and occ_{svp} for each speed bin. Lane 1 with the time-of-day HOV restriction clearly shows the sympathy of speeds and lower vehicular throughput compared to the GP Lane 2. This outcome is similar to the past operational findings discussed in Section 2.1. These qoccFR curves are then projected into qkFR in Fig. 1b and then VXp in Fig. 1c via Equations 5-6. Indeed from the VXp plot it is clear that the HOV lane exhibits longer spacing for a given speed compared to the GP lane. It is also worth noting that (i) both the qoccFR and qkFR

[3] For completeness, note that buses are allowed in both lanes and the occasional truck does pass illegally in these lanes.
[4] Although not shown, well over 95% of the vehicle lengths in each lane fall between 15 and 30 ft during both the HOV and separately the non-HOV periods.

exhibit a roughly triangular shape in the GP lane and a roughly parabolic shape in the HOV lane, and (ii) the HOV lane's parabolic curve falls completely inside the GP lane's triangular curve.

To avoid potentially mixed traffic conditions that exhibit behaviors from both the free flow and congested regimes the focus of this study is primarily congested flows below the apparent vehicular capacity. To underscore this fact while also facilitating comparison across different plots and coordinate systems, two different styles of dashed lines are used to denote 40 mph and 50 mph thresholds. As noted in Section 2.3, when binning by speed the performance of the svp method is expected to degrade outside of the congested regime. While there is not a crisp boundary between the strictly car following of the congested regime and mixed traffic in the transition region to free flow, this work presumes the upper limit of the strictly car following behavior falls somewhere between 40 and 50 mph on this freeway with a 65 mph speed limit. The reader can choose which reference line they prefer to use for comparisons across figures and plots.

Thus far the discussion has been too simplistic because it blindly combines very different traffic conditions together: lane 1 is a time-of-day HOV lane that reverts to a GP lane during the non-HOV periods. Two distinct peaks are clearly evident for lane 1 in Fig. 1a, with the left peak from GP vehicles during non-HOV hours and the right peak from HOV vehicles during HOV hours. To avoid potential confusion between the HOV lane itself and the periods when the HOV restriction is active, henceforth this paper will refer to the lanes by their number: with lane 1 being the time-of-day HOV lane and lane 2 being the GP lane.

The operational relationships of HOV lanes had previously only been studied on HOV facilities that were active 24 hrs/day or strictly during the periods when a time-of-day HOV restriction was active. As the first step beyond the past work discussed in Section 2.1, the current work uses a time-of-day HOV lane and explicitly considers the non-HOV conditions distinct from the HOV conditions. The top row of plots in Fig. 2 shows the qoccFR, qkFR and VXp for lane 1 separately for the HOV and non-HOV periods. Compared to Fig. 1, the two curves are much further apart in each of the plots even though in Fig. 2a-c the curves come from the same lane. Clearly, upon isolating the HOV operations the reduced vehicular throughput and increased spacing associated with HOV operations become more pronounced. On the other hand, during the non-HOV period lane 1 reverts to GP operations and the resulting curves look very similar to those from lane 2 in Fig. 1, e.g., exhibiting a much higher vehicular throughput and nearly triangular shape in the qkFR.

Repeating this analysis in lane 2, as shown in Fig. 2d-f, there is very little change in the strictly GP lane between the HOV and non-HOV periods. Within the congested regime Fig. 2d-e show that in lane 2 there is a slight move towards higher density or occupancy at a given value of flow during the HOV period compared to the non-HOV period. This trend suggests that perhaps the aggressive drivers who would normally be in lane 1 but do not meet the HOV requirement are traveling in lane 2 during the HOV period. Finally, the bottom row of plots compare the two lanes during the non-HOV period, showing that the two lanes behave very similarly when the HOV restriction is inactive. Fig. 2g-i show that during the non-HOV period that lane 1 falls above lane 2 in the qoccFR and qkFR, or in the VXp plane lane 1 falls to the left of lane 2. These trends are the opposite of those found in Fig. 1, where the HOV period contributes most of the congested data. Using the non-HOV curves for lane 2 as a common reference in the bottom two rows of plots, a given non-HOV period curve from lane 1 is similar to the corresponding HOV period curve from lane 2, suggesting that indeed during the non-HOV period the aggressive drivers that do not meet the HOV restriction are able to travel in lane 1 instead of lane 2.

While there is clearly a correlation between the unusual relationships in lane 1 and the HOV period, at this point one should resist the temptation to attribute the unusual relationships as being an intrinsic characteristic of HOV operations. One cannot assume that the unusual behavior in lane 1 arises independent of other factors. In general, one would expect any congestion to first manifest in the GP lanes, with the HOV lane potentially remaining in the free flow regime. If conditions worsen to the point where the HOV lane sees reduced speed, it is quite likely that the GP lanes are experiencing even lower speed[5], see, e.g., Jang and Cassidy (2012). Simply measuring the relationships in a single lane without accounting for the concurrent conditions in the other lanes can obscure causal relationships.

To account for the concurrent conditions this work explicitly measures the relative speed between lanes. As noted in Coifman (2015), if other explanatory variables are measured or otherwise become available, the svp method can be extended to account for them via additional dimensions in the sampling bins. So to capture the inter-lane relationships, this work extends the svp method applied to lane 1 by adding a third dimension to the binning process: also sorting vehicles based on relative speed from lane 1 to lane 2. The relative speed, Δv_{12}, is calculated via Equation 7, where v_1 is the current v_{svp} in lane 1 and v_2 is the immediately preceding v_{svp} in lane 2.

$$\Delta v_{12} = v_1 - v_2 \tag{7}$$

Revisiting the lane 1 curve in Fig. 2b-c from the HOV period, Fig. 3 shows the same data only now binned by Δv_{12} into 10 mph bins. Given the redundancy between qoccFR and qkFR curves for a given L_{eff}, this plot only shows the qkFR, and given the fact that the performance of the svp method is expected to degrade outside of the congested regime the plotted data are now limited to $v_1 < 50\ mph$. The top row of plots in Fig. 3 uses solid lines to show the three Δv_{12} bins spanning -10 mph to 20 mph while the bottom row shows the three Δv_{12} bins spanning 20 mph to 50 mph. For reference, the two original curves from the respective subplot in Fig. 2b-c are repeated with points in all four of these plots. The lowest Δv_{12} bin in Fig. 3a-b corresponds to the situation where lane 1 is moving slower than lane 2. Indeed, in this situation the qkFR and VXp from the HOV period are almost indistinguishable from the reference curve from Fig. 2b-c for the non-HOV period. The next two Δv_{12} binned curves come from when lane 1 is moving faster than lane 2, with the 10-20 mph bin nearly falling on top of the original curve for the HOV period without any binning by Δv_{12} (i.e., the reference curve from Fig. 2b-c); and the 0-10 mph curve falling a little above the 10-20 mph curve. Fig. 3c-d show that as Δv_{12} becomes larger the corresponding curve moves further down in the plots relative to the other curves. Again, all of these curves come from the HOV period except for the one non-HOV reference curve that is repeated from Fig. 2b-c. Clearly the fact that the HOV restriction is active does not on its own explain the wide range of behavior across the different Δv_{12} bins, whereas the evolution of curves in the VXp plots of Fig. 3b and Fig. 3d clearly shows that as Δv_{12} increases, the lane 1 drivers become more conservative by taking a longer spacing for a given speed (or lower speed for a given spacing).

These clean results arise because the extended svp method takes each vehicle individually and then groups them into homogeneous bins based on length, speed, and relative speed. The homogeneity extends to each dimension of the binning process. So in the extended svp all

[5] Although for brevity the time series results are not shown, upon examining the time series speeds across lanes when the segment was congested during the HOV period we did in fact observe that the GP lane typically exhibited speeds below those in the HOV lane.

vehicles in a given bin have the same relative speed to the adjacent lane. This influence is usually washed away in conventional macroscopic measurements that arbitrarily group inhomogeneous vehicles together based on arrival order. This fact is important, because by preserving the influence of the relative speed to the adjacent lane with the homogeneous bins like this, one can now examine the impact of relative speed during the non-HOV period too, i.e., when lane 1 operates as a GP lane. Fig. 4 repeats the analysis from Fig. 3 in lane 1 except now strictly using data from the non-HOV period. There were only three Δv_{12} bins that had enough samples to provide cohesive curves (recall that this work requires a minimum of 100 vehicles per speed bin). The general trend from Fig. 3 repeats itself here, as Δv_{12} increases the qkFR and VXp curves move lower. The highest Δv_{12} bin, 10-20 mph, only has sufficiently large samples when v_1 is above 38 mph. In this small range the curve approaches the general shape that was previously seen in Fig. 2b-c during the HOV period. Comparing Fig. 4 to the top row in Fig. 3, the Δv_{12} bins are the same. Yet the curve for a given Δv_{12} bin in the non-HOV period of Fig. 4 generally falls above the corresponding curve for the same Δv_{12} bin in the HOV period of Fig. 3. Looking closer at this range, the left-hand column of plots in Fig. 5 repeats the analysis in the VXp plane only now using 5 mph Δv_{12} bins. First, for reference Fig. 5a repeats Fig. 2c for the case without binning by Δv_{12}. The curves in lane 1 for HOV and non-HOV periods are about 40 ft apart when $v_1 \approx 50\ mph$ and remain above 10 ft apart until $v_1 < 30\ mph$. Yet as shown in Fig. 5b these large differences in median spacing also correspond to a large difference in mean Δv_{12}, with the mean Δv_{12} above 10 mph until $v_1 < 30\ mph$. Note that in the plots on the right hand side of Fig. 5 the independent variable is plotted on the ordinate to facilitate comparison with the VXp plot.

Next, consider the results for the Δv_{12} binned data. With the 5 mph Δv_{12} bins there are only 4 bins with a sufficient number of samples in both the HOV and non-HOV periods, as shown in the bottom four rows of plots in Fig. 5. The left hand column of plots show that the curves in the VXp plane have moved much closer together compared to Fig. 5a. Fig. 6 shows the difference in spacing for a given v_1 between the HOV and non-HOV periods, with one curve for each of the three lowest Δv_{12} bins. Like Fig. 5b, the independent variable is plotted on the ordinate to facilitate comparison with the VXp plot. The Δv_{12} binned data are denoted with lines in Fig. 6. For reference the points show the difference between the HOV and non-HOV curves in the case without binning by Δv_{12} (i.e., Fig. 5a). Clearly the difference in spacing for the binned data is much closer to zero across almost all v_1 and Δv_{12}. The 5 mph bins have moved the curves closer than what was found without binning by Δv_{12} (and what was found in the 10 mph bins[6]) but Fig. 6 shows that generally a non-zero difference persists between the spacing seen in the HOV and non-HOV periods for a given v_1 and Δv_{12}, and it does so with a positive bias. The (tighter) binning moves the comparison closer to that of similar underlying conditions, but differences remain. Consider Fig. 5d, 5f, 5h, and 5j: in each plot the horizontal range corresponds to the span of the given Δv_{12} bin, with a vertical line denoting the center of the bin. The points show the mean Δv_{12} at the given v_1 under each condition. Generally the mean Δv_{12} from the non-HOV data fall a few mph to the left of the corresponding HOV data, indicating that a small bias remains in the underlying data.

[6] For brevity the spacing difference for Δv_{12} 10 mph bins are not explicitly shown in this paper, but the larger spacing seen in the larger Δv_{12} bins can be extrapolated by comparing the VXp curves Fig. 3 and Fig. 4.

3.2.1. The Influence of Recent History

Thus far the analysis does not consider the recent history experienced by the drivers. Prior work has shown that drivers take up to 30 sec to *relax* to changing conditions in the presence of lane change maneuvers (e.g., Wang and Coifman, 2008; Xuan and Coifman, 2012). Although only a hypothesis at this time, we suspect that drivers also relax to changing conditions as Δv_{12} evolves. Since Δv_{12} can change rapidly, if a driver's spacing at time t_0 depends on $\Delta v_{12}(t_0)$ the spacing probably also depends on $\Delta v_{12}(t_0 - \tau)$ as experienced for the previous several τ seconds, reflecting the driver's relaxation process. The analysis in this paper only uses the instantaneous Δv_{12} and thus far the work has made no attempt to capture the fact that Δv_{12} might be changing rapidly enough that the drivers did not have time to completely relax to the given Δv_{12}. Simply from the range of Δv_{12} bins in Fig. 3 and 4 it is clear that during the HOV period that on average the lane 1 drivers see higher $\Delta v_{12}(t_0)$ than the non-HOV period. Presumably this relationship also applies to the recent history, i.e., $\Delta v_{12}(t_0 - \tau)$ should on average be higher in the HOV period than the non-HOV period. Fully testing this hypothesis is the subject of on-going research, though as partial motivation for this view, Fig. 7a-d tallies the proportion of times that the traffic state enters a given Δv_{12} bin from a higher Δv_{12} bin for the HOV and non-HOV periods (with the rest entering from a lower bin), while Fig. 7e-h repeat the tallies for leaving a given Δv_{12} bin. For example, Fig. 7c shows that during the HOV period roughly 75% of the times that the Δv_{12} enters the 5-10 mph bin it does so from a higher Δv_{12} bin, and thus, only 25% of the time from a lower Δv_{12} bin.[7] Fig. 7c also shows that during the non-HOV period, the rates reverse for the 5-10 mph Δv_{12} bin, with the state usually entering from a lower Δv_{12} bin. Fig. 7g shows similar rates for when the traffic state leaves the 5-10 mph Δv_{12} bin. Thus, assuming that the recent history of $\Delta v_{12}(t_0 - \tau)$ influences behavior in the same direction as $\Delta v_{12}(t_0)$, but to a lesser magnitude, the drivers in a given $\Delta v_{12}(t_0)$ bin will generally see a higher $\Delta v_{12}(t_0 - \tau)$ in the HOV period than in the non-HOV period.

For this discussion τ is simply used as shorthand to denote that some unknown amount of the recent past is important, and we suspect the critical Δv_{12} is as seen from the driver's perspective, i.e., speeds experienced upstream of the detector station. In practice we suspect this impact would take the form of a weighted average of Δv_{12} over some range of time and space. The time span might be on the order of observed relaxation times after a lane change maneuver (e.g., as discussed in Wang and Coifman, 2008; Xuan and Coifman, 2012), or it might be longer before a driver feels comfortable taking a shorter spacing. What we do know is that since the HOV period drivers in a given $\Delta v_{12}(t_0)$ bin will generally see a higher $\Delta v_{12}(t_0 - \tau)$ than in the non-HOV period, whatever functional form the relaxation relation may take, the HOV period drivers should exhibit a greater acclimation to high Δv_{12} than the non-HOV period drivers. So in an effort to partially capture the difference in $\Delta v_{12}(t_0 - \tau)$ between the HOV and non-HOV periods, first Fig. 8 repeats the comparisons of Fig. 5c, 5e and 5g. Since the non-HOV period generally has $\Delta v_{12}(t_0 - \tau)$ from lower bins while the HOV period generally has $\Delta v_{12}(t_0 - \tau)$ from higher bins, Fig. 8 adds the VXp curve from the next higher Δv_{12} bin during the non-HOV period. In each plot the VXp curve from the HOV period is much closer to VXp curve from the higher Δv_{12} bin during the non-HOV period than it is to the VXp curve from the same Δv_{12} bin

[7] So in this case if the first of five successive vehicles fell in the 10-15 Δv_{12} bin, the next three vehicles fell in the 5-10 mph Δv_{12} bin, and the final vehicle fell in the 0-5 mph Δv_{12} bin, then the three successive 5-10 mph Δv_{12} bin vehicles would contribute a single "entrance" event and a single "exit" event. In this case the entrance would be from a higher Δv_{12} bin and the exit to a lower Δv_{12} bin.

during the non-HOV period. Thus, suggesting that indeed the recent history (as expressed by the previous Δv_{12} bin) also influences the driver's behavior.

3.2.2. The influence of acceleration

The current work does not attempt to account for acceleration; either over the dual loop detector or after a given vehicle passes the detector. This unobserved acceleration will undoubtedly impact the true spacing, as opposed to the estimated spacing from Equation 6 used in this work. At the moment there is no obvious way to accurately measure individual vehicle acceleration over space with only a dual loop detector. Instead of relying strictly on individual measurements this work requires a minimum of 100 vehicles per bin. Inevitably a few vehicles among the individual svp data will exhibit large errors in one direction due to decelerations and large errors in the other direction due to accelerations; however, these large errors will fall on the tails of the distribution. By taking the median across all of the svp data a given bin the impact of the outliers should be minimized when finding the central tendency; thus, clipping off most of the impacts of acceleration and deceleration. In any event the impacts of acceleration increase as speeds decrease. Wu and Coifman (2014) found that the impacts on individual vehicle measurements only become an issue below 10 mph, while most of the results in this study come from traffic with speeds above 20 mph. To support these suppositions, Fig. 2c shows that the HOV and non-HOV curves converge as speed drops, and similarly Fig. 3 and Fig. 4 show that the curves across different relative speed bins converge as speed drops. If acceleration were an important factor the curves should not converge like this. Further discussion of how accelerations impact the svp can be found in Coifman (2015). Finally, note that the unobserved acceleration will also impact conventional measures of flow and occupancy, but under conventional aggregation the noise from the inhomogeneous vehicle fleet and measurement errors are far greater than the noise due to unaccounted for acceleration.

3.3. Fitting regression curves to the observed VXp

This section begins to model the dependency on the relative speed between lanes by fitting linear regression curves to the empirical data. To facilitate the use in car following models all of the regression models this section follow the conventional practice from the car following literature where spacing is the dependent variable and speed the explanatory variable (e.g., Gazis et al., 1961; Newell, 2002). Treating the non-HOV and HOV periods separately, Fig. 9a fits linear curves in the form of Equation 8 to the three non-HOV Δv_{12} bins used in Fig. 4 while Fig. 9b does so with parabolic curves in the form of Equation 9; where Xp is spacing, v is speed, and a, b, c, d are e are the coefficients. Note that the axes in Fig. 9 have been transposed from Fig. 4b, reflecting the conventional car following assumption that spacing depends on speed. The resulting statistics are presented in Table 2. Fig. 10 repeats this analysis for the six HOV Δv_{12} bins used in Fig. 3. In Fig. 10 the left column of plots show the fitted linear curves and right column of plots show the fitted parabolic curves. The resulting statistics for the HOV period are presented in Table 3.

$$\mathrm{Xp} = a + b * v \tag{8}$$

$$\mathrm{Xp} = c + d * v + e * v^2 \tag{9}$$

Both by inspection of Fig. 9 and via the adjusted R^2 the fitted linear curves appear to be at least as good as the corresponding parabolic curve fit to each of the three non-HOV Δv_{12} bins. On the other hand, Table 3 shows that the adjusted R^2 for the fitted parabolic curves is always

higher than that of the corresponding linear curve fit for all six of the HOV Δv_{12} bins. In both the non-HOV and HOV curves the highest Δv_{12} bin has only 4 samples while all other bins have at least 10 samples, hence, the fitted curves for these highest Δv_{12} bins should be viewed with greater caution. Formalizing these comparisons, F-tests were conducted for the different Δv_{12} bins separately during the non-HOV and the HOV periods. In the context of these tests, the linear curve with one explanatory variable is the reduced model and the parabolic curve with two explanatory variables is the full model. The null hypothesis H_0 was that the quadratic term can be dropped, i.e., $e = 0$, and the alternative hypothesis H_a was that $e \neq 0$. The F-test essentially checks if the inclusion of quadratic term leads to a decrease in the sum of the squared errors of the model. For the non-HOV period Table 4 shows that the linear curve model would be sufficient for all three of the Δv_{12} bins. On the other hand for the HOV period Table 5 shows that the parabolic curve model is a better fit for all six of the Δv_{12} bins.

4. Discussion and Conclusions

Past studies in traffic operations have observed macroscopically that HOV lanes exhibit markedly different dynamics than the adjacent GP lanes, with the HOV lanes exhibiting lower flows than the GP lanes at speeds throughout the congested regime. This paper examined the microscopic traffic relationships to better understand the car following behavior underlying the phenomena. This work studied a time-of-day HOV lane using the single vehicle passage (svp) method. During the non-HOV periods the study lane reverts to a GP lane, thereby providing a control condition for the specific lane and location. The research showed that when the HOV restriction was inactive that indeed the time-of-day HOV lane exhibited behavior similar to the GP lanes; thus, the unusual HOV relationships were not specifically related to the geometry of the site. After extending the svp method to also account for relative speed to the adjacent lane, Δv_{12}, it was shown that the simple fact that the HOV restriction is active does not explain the wide range of behavior across the different Δv_{12} bins, whereas the evolution of curves in the speed spacing relationship (VXp) of Fig. 3b and Fig. 3d clearly shows that as Δv_{12} increases, the HOV drivers in lane 1 become more conservative by taking a longer spacing for a given speed (or lower speed for a given spacing). For reference, Section 3.3 fit regression curves to the observed VXp data within the different Δv_{12} bins.

The extended svp method allowed this work to also analyze the influence of Δv_{12} when the HOV restriction was inactive and the study lane served GP vehicles. By taking care to preserve the influence of the relative speed to the adjacent lane during the non-HOV period this work shows that the dependency on the adjacent lane persists during the GP operations (Fig. 4). In other words the car following behavior that gives rise to the sympathy of speeds is unrelated to the HOV restriction per se, since the sympathy of speeds is also observed under GP operations. This finding is important since most existing car following models assume that the longitudinal acceleration of a following vehicle is strictly a function of speed and spacing to the leading vehicle in the same lane. Because drivers in general adopt a larger spacing when faced with a high differential in speed between lanes this finding means that actual car following behavior also depends on the relative speed to the adjacent lane. This fact has likely gone unnoticed in GP lanes to date because generally the conditions that give rise to a differential in speeds between lanes are usually short lived, and thus, do not become apparent in conventional macroscopic data that arbitrarily group inhomogeneous vehicles together based on arrival order. In such sequential grouping the influence from a sympathy of speeds is obscured due to rapidly

changing conditions except under exceptional circumstances that include confounding factors like HOV operations where the differential in speed arising from the priority vehicles can be sustained for extended time periods.

We suspect these confounding factors have also impacted many of the previous macroscopic studies of the vehicular capacity of HOV lanes. While those studies measured the maximum throughput in the HOV lane and found it to be far lower than the apparent capacity of the adjacent GP lanes, it is our suspicion that the maximum throughput was not the actual capacity of the HOV lane. Instead, an HOV lane is rarely able to exhibit capacity flow because demand for the lane only arises when the adjacent GP lanes are traveling at much slower speeds and thus, the large relative speed pulls the HOV flow down from the capacity that lane could otherwise exhibit (see, e.g., the top row of plots in Fig. 2). From an operations standpoint it may be appropriate to equate maximum observed throughput as being the effective capacity since it inherently accounts for the coupling factors that are regularly observed across lanes. However, from the traffic flow theory standpoint the distinction between maximum observed flow and the vehicular capacity is an important one to make, allowing for a deeper understanding of the underlying traffic dynamics.

Although this work used the extended svp method to isolate the relative speed between lanes, there are many other factors that are suspected to influence behavior too, e.g., acceleration or lane change maneuvers. There is certainly long standing evidence that acceleration impacts driver behavior, e.g., Newell (1965) developed a model to capture the observed phenomena wherein drivers take longer gaps when accelerating than when they are decelerating. As discussed in Section 3.2.2, the extended svp method developed herein minimizes the impacts of acceleration. Similarly, lane change maneuvers are difficult to measure from loop detector data; however, when there is a high relative speed between two lanes there should be few lane change maneuvers between those two lanes. Generally speaking, for a lane change to occur in congested traffic the two lanes have to have relatively similar speeds so that a driver can adopt the new lane's speed in the gap they just accepted. Like the discussion of acceleration, there will undoubtedly be occasional exceptions, but these impacts will fall on the tails of the svp distribution in a given bin and should generally have little impact on the central tendency as measured by the median values of that bin. In the long run studying the deviations from the central tendency due to acceleration, lane change maneuvers, and other factors will be of great interest, but those topics are left to future research.

Finally, while this work did observe the sympathy of speeds in the study lane under GP operations, even after accounting for the instantaneous Δv_{12} small differences remain between the HOV and non-HOV relationships. It was hypothesized that there is also a relaxation factor with a longer time constant as the drivers acclimate to a long-standing differential in relative speeds (HOV) or only experience transient disturbances (GP).

Acknowledgements

This material is based upon work supported in part by Ohio State University's Crash Imminent Safety (CrIS) a USDOT Tier I University Transportation Center. The contents of this report reflect the views of the authors who are responsible for the facts and the accuracy of the data presented herein. The contents do not necessarily reflect the official views or policies of the Federal Highway Administration. This report does not constitute a standard, specification or regulation.

The authors also appreciate the constructive input from the anonymous reviewers. Their input has helped make this a better paper.

References

Bando, M., Hasebe, K., Nakayama, A., Shibata, A., Sugiyama, Y. (1995) “Dynamical Model of Traffic Congestion and Numerical Simulation”, Physical Review E, Vol. 51, No. 2, pp. 1035-1042

Chandler, R. E., Herman, R., Montroll, E. W. (1958) “Traffic Dynamics: Studies in Car Following”, Operations Research, Vol. 6, pp. 165-184.

Coifman, B. (2001) “Improved Velocity Estimation Using Single Loop Detectors”, Transportation Research: Part A, Vol. 35, No 10, pp. 863-880.

Coifman, B. (2014a) "Jam Occupancy and Other Lingering Problems with Empirical Fundamental Relationships," Transportation Research Record 2422, pp. 104-112.

Coifman, B. (2014b) “Revisiting the Empirical Fundamental Relationship”, Transportation Research- Part B, Vol. 68, pp. 173-184.

Coifman, B. (2015) “Empirical Flow-Density and Speed-Spacing Relationships: Evidence of Vehicle Length Dependency”, Transportation Research- Part B, Vol. 78, pp. 54-65.

Coifman, B., Kim, S. (2011) "Extended Bottlenecks, the Fundamental Relationship and Capacity Drop," Transportation Research- Part A. Vol. 45, No 9, pp. 980-991.

Coifman, B., Lyddy, D., Skabardonis, A. (2000) “The Berkeley Highway Laboratory- Building on the I-880 Field Experiment”, Proc. IEEE ITS Council Annual Meeting, IEEE, pp. 5-10.

Coifman, B., Wang, Y. (2005) "Average Velocity of Waves Propagating Through Congested Freeway Traffic," Proc. of The 16th International Symposium on Transportation and Traffic Theory, July 19-21, 2005, College Park, MD, pp. 165-179.

Evans, L., Rothery, R. (1973) “Experimental Measurement of Perceptual Thresholds in Car Following”, Highway Research Record, No. 464, pp. 13-29.

Evans, L., Rothery, R. (1977) “Perceptual Thresholds in Car Following: a Recent Comparison”, Transportation Science, Vol. 11, No. 1, pp. 60-72.

Fellendorf, M., Hoyer, R. (1997) “Parameterization of Microscopic Traffic Models through Image Processing”, Proc. of the IFAC Transportation System Conference, Chania, Greece, pp. 929-934.

Gazis, D. C., Herman, R., Potts, R. B. (1959) “Car Following Theory of Steady State Traffic Flow”, Operations Research, 7, pp. 499-505.

Gazis, D. C., Herman, R., Rothery, R. W. (1961) “Nonlinear Follow the Leader Models of Traffic Flow”, Operations Research, 9, pp. 545-567.

Ge, H.X., Dai, S.Q., Dong, L.Y., Xue, Y. (2004) “Stabilization Effect of Traffic Flow in an Extended Car-following Model based on an Intelligent Transportation System Application”, Physical Review E, Vol. 70, No. 066134, pp. 1-6.

Gipps, P.G. (1981) “A Behavioral Car Following Model for Computer Simulation” Transportation Research Part B (15), pp. 105–111.

Guin, A., Hunter, M. P., Guensler, R. L. (2008) “Analysis of Reduction in Effective Capacities of High-Occupancy Vehicle Lanes related to Traffic Behavior”, Transportation Research Record, No. 2065, pp. 47–53.

Gunay, B. (2007) “Car Following Theory with Lateral Discomfort”, Transportation Research – Part B, Vol. 41, No. 7, pp. 722-735.

Herman, R., Potts, R.B. (1959) “Single Lane Traffic Theory and Experiment”, Proc. of the Symposium on Theory of Traffic Flow, Elsevier, New York, pp. 147-157.

Jang, K., Cassidy, M. (2012) “Dual influences on vehicle speed in special-use and critique of US regulation”, Transportation Research - Part A, 46, pp. 1108-1123.

Jang, K., Oum, S., Chan, C. (2012) “Traffic Characteristics of High-occupancy Vehicle Facilities: Comparison of Contiguous and Buffer-separated Lanes”, Transportation Research Record, No. 2278, pp. 180–193.

Jin, S., Wang, D.H., Huang, Z.Y., Tao, P.F., Li, P. (2010) “Non-lane-based Full Velocity Difference Car Following Model”, Physica A: Statistical Mechanics and its Applications, Vol. 389, No. 21, pp. 4654-4662.

Jin, S., Wang. D.H., Huang, Z.Y., Tao, P.F. (2011a) “Visual Angle Model for Car-following Theory”, Physica A: Statistical Mechanics and its Applications, Vol. 390, No. 11, pp. 1931–1940.

Jin, S., Wang, D.H., Xu, C., Huang, Z. (2012) “Staggered Car-following Induced by Lateral Separation Effects in Traffic Flow”, Physics Letters A, Vol. 376, No. 2, pp. 153-157.

Jin, S., Wang, D.H., Yang, X. (2011b) “Non-lane-based Car-following Model using Visual Angle Information”, Transportation Research Record, No. 2249: pp. 7-14.

Kim, S., Coifman, B., (2013) "Driver Relaxation Impacts on Bottleneck Activation, Capacity, and the Fundamental Relationship," Transportation Research- Part C, Vol 36, pp. 564-580.

Kometani, E., Sasaki, T. (1958) “On the Stability of Traffic Flow”, Journal of Operations Research Society Japan, Vol. 2, pp. 11-26.

Kumamoto, H., Nishi, K., Tenmoku, K., & Shimoura, H. (1995) “Rule based Cognitive Animation Simulator for Current Lane and Lane Change Drivers”, Proc. of the Second World Congress on ITS, Yokohama, Japan, Vol. 4, pp. 1746-1752.

Lee, D. N. (1976) “A Theory of Visual Control of Braking based on Information about Time to Collision”, Perception, Vol. 5, pp. 437-459.

Lee, J., Jones, J.H. (1967) “Traffic Dynamics: Visual Angle Car Following Models”, Traffic Engineering and Control, Vol. 8, No. 8, pp. 348-350.

Lenz, H., Wagner, C. K., Sollacher, R. (1999) “Multi-anticipative Car-following Model”, The European Physical Journal B- Condensed Matter and Complex Systems, Vol. 7, No. 2, pp. 331-335.

Leutzbach, W., Wiedemann, R. (1986) “Development and Applications of Traffic Simulation Models at the Karlsruhe Institut fur Verkehrwesen”, Traffic Engineering and Control, Vol. 27, No. 5, pp. 270-278.

Liu, M.Y., Di, H.H., Yu, X., Wei, S., Zhen, L.W. (2008) “Effect of Multi-velocity-difference in Traffic Flow”, Chinese Physics B, Vol 17, No 12, pp. 4446-4450.

Liu, X., Schroeder, B., Thomson, T., Wang, Y., Rouphail, N., Yin, Y. (2011) “Analysis of Operational Interactions between Freeway Managed Lanes and Parallel, General Purpose Lanes”, Transportation Research Record, No. 2262, pp. 62-73.

Liu, X., Zhang, G., Lao, Y., Wang, Y. (2012) “Modeling Traffic Flow Dynamics on Managed-Lane Facility: Approach Based on Cell Transmission Model”, Transportation Research Record, No. 2278, pp. 163-170.

Luo, Y., Boloni, L. (2012) “Modeling the Conscious Behavior of Drivers for Multi-lane Highway Driving”, Proc. of the 7th Workshop on Agent in Traffic and Transportation, pp. 95-103.

Manda, H., Song, Z., Yin, Y., Wang, Y. (2011) “Comparison of Capacities of High- Occupancy Vehicle and General Purpose Lanes”, Proc. of 90th Annual Meeting of the Transportation Research Board, Washington, D.C.

Martin, P., Perrin, J., Lambert, R., Wu, P. (2002) “Evaluate Effectiveness of High Occupancy Vehicle (HOV) Lanes”, University of Utah, Salt Lake City; Utah Department of Transportation, 51 p.

Michaels, R.M. (1963) “Perceptual Factors in Car Following”, Proc. of the Second International Symposium on the Theory of Road Traffic Flow, Paris, pp. 44-59.

Montroll, E.W. (1959) “Acceleration and Clustering Tendency of Vehicular Traffic”, Proc. of the Symposium on Theory of Traffic Flow, Elsevier, New York, pp. 147-157.

Nagatani, T. (1999) “Stabilization and Enhancement of Traffic Flow by the Next-nearest-neighbor Interaction”, Physical Review E, Vol. 60, No. 6, pp. 6395-6401.

Newell, G. (1965) "Instability in dense highway traffic", Proc. 2nd International Symposium on the Theory of Road Traffic Flow, pp 73-83

Newell, G. (2002) "A simplified car-following theory: a lower order model", Transportation Research Part B, Vol. 36, 2002, pp. 195-205.

Peng, G.H., Sun, D.H. (2010) “A Dynamical Model of Car-following with the Consideration of the Multiple Information of Preceding Cars”, Physics Letters A, Vol. 374, No.15-16, pp. 1694–1698

Reiter, U. (1994) “Empirical Studies as Basis for Traffic Flow Models”, Proc. of the Second International Symposium on Highway Capacity, pp. 493-502.

Sauer, C.W., Andersen, G. J., Saidpour. A. (2003) “Car Following by Optical Parameters”, Proc. of the Second International Driving Symposium on Human Factors in Driver Assessment, Training and Vehicle Design, pp. 158-162.

Tang, T.Q., Huang, H. J., Gao, Z. Y. (2005) “Stability of the Car-following Model on Two Lanes”. Physical Review E, 72, No. 066124, pp. 1- 7.

Thomson, T., Liu, X., Wang, Y., Schroeder, B. J., Rouphail, N. M. (2012) “Operational Performance and Speed–Flow Relationships for Basic Segments of Managed-Lane Segments”, Transportation Research Record, No: 2286, pp. 94-104.

Treiber, M., Hennecke, A., Helbing, D. (2000) “Congested traffic states in empirical observations and microscopic simulations”, Physical Review E, Vol. 62, pp. 1805–1824.

Treiber, M., Kesting, A. (2009) “Modeling Lane-changing Decisions with MOBIL”, Proc. of Traffic and Granular Flow ‘07, pp. 211–221.

Wang, C., Coifman, B. (2008) “The Effect of Lane Change Maneuvers on a Simplified Car-following Theory”, IEEE Transactions on Intelligent Transportation Systems, Vol 9, No. 3, pp. 523-535.

Wilson, R.E., Berg, P., Hooper, S., Lunt, G. (2004) “Many-neighbor Interaction and Non-locality in Traffic Models”, European Physical Journal B- Condensed Matter and Complex Systems, Vol. 39, No. 3, pp. 397-408.

Wu, L., Coifman, B. (2014) "Vehicle Length Measurement and Classification in Congested Freeway Traffic," Transportation Research Record 2443, pp. 1-11.

Xu, G., Huang, X. P., Pant, P. (1999) “Method for Estimating Capacity Reduction in High-Occupancy-Vehicle Lane Ingress and Egress Sections”, Transportation Research Record, No. 1678, pp. 107–115.

Xuan, Y., Coifman, B. (2012) “Identifying Lane Change Maneuvers with Probe Vehicle Data and an Observed Asymmetry in Driver Accommodation”, Journal of Transportation Engineering, ASCE, Vol. 138, No. 8, pp. 1051-1061.

List of Tables

List of Figures

Table 1, Total number of vehicles seen over 69 weekdays, sorted by indicated criteria, as used in this study.

Description	Length range (ft)	Lane 1: time of day HOV (# veh)	Lane 2: GP (# veh)
all hours(0-24 hours)	all	4,814,828	9,552,639
all hours(0-24 hours)	18-22	3,444,869	7,139,764
HOV hours (lane 1 HOV)	18-22	1,057,949	1,759,759
HOV hours with speeds < 40 mph	18-22	122,899	1,069,379
HOV hours with speeds < 50 mph	18-22	440,545	1,389,218
HOV hours with speeds < 65 mph	18-22	972,230	1,718,563
Non-HOV hours (lane 1 GP)	18-22	1,048,498	1,392,355
Non-HOV hours with speeds < 40 mph	18-22	16,985	20,060
Non-HOV hours with speeds < 50 mph	18-22	33,851	41,689
Non-HOV hours with speeds < 65 mph	18-22	213,703	716,906

Table 2, Regression analysis results for VXp in lane 1 during the non-HOV period.

v12 bin, mph	Linear models				Non-linear models					# samples
	Model Specification, Xp = a + b*v				Model Specification, Xp = c + d*v + e*v^2					
	a	b	R^2	Adj.R^2	c	d	e	R^2	Adj.R^2	
-10 to 0	25.083	1.590	0.977	0.976	26.716	1.480	0.002	0.977	0.975	20
0 to 10	28.518	1.697	0.989	0.988	33.264	1.359	0.005	0.989	0.989	25
10 to 20	30.540	1.922	0.835	0.752	463.488	-17.588	0.219	0.885	0.654	4

Table 3, Regression analysis results for VXp in lane 1 during the HOV period.

v12 bin, mph	Linear models				Non-linear models					# samples
	Model Specification, Xp = a + b*v				Model Specification, Xp = c + d*v + e*v^2					
	a	b	R^2	Adj.R^2	c	d	e	R^2	Adj.R^2	
-10 to 0	25.273	1.746	0.976	0.975	37.770	0.729	0.018	0.989	0.988	25
0 to 10	26.665	1.922	0.985	0.985	42.420	0.705	0.021	0.997	0.997	29
10 to 20	17.036	2.371	0.981	0.980	54.523	-0.046	0.036	0.996	0.996	22
20 to 30	0.584	2.935	0.979	0.977	59.609	-0.502	0.048	0.989	0.988	17
30 to 40	-27.880	3.708	0.973	0.969	132.776	-4.558	0.104	0.990	0.987	10
40 to 50	-114.004	5.719	0.976	0.964	716.274	-31.697	0.420	1.000	1.000	4

Table 4, Test of Linearity for the VXp regression in lane 1 during the non-HOV period.

v12 bin, mph	# samples	SSR(Xp^2|Xp)	Num. df	SSE(Xp^2,Xp)	Den. df	Test statistic	F critical	p-value	Result
-10 to 0	20	0.433	1	86.241	17	0.085	4.451	0.774	FTR
0 to 10	25	5.528	1	64.297	22	1.891	4.301	0.183	FTR
10 to 20	4	6.410	1	14.812	1	0.433	161.448	0.630	FTR

Where

SSR (Xp^2|Xp) = difference in regression sum of squares between the full and the reduced models
Num. df = Numerator degrees of freedom
SSE (Xp^2, Xp) = Sum of squared errors for the full model
Den. df = Denominator degrees of freedom
Test Statistic = F-value calculated for a given dataset
F critical = Critical value of the F distribution
p-value = smallest value of alpha for rejecting H_0 (reject H_0 if p-value < α)
Result = Test result
FTR = Test failed to reject the null hypothesis that e = 0

Note: A significance level of 0.05 has been fixed as α for the F-tests

Table 5, Test of Linearity for the VXp regression in lane 1 during the HOV period, using the same notation as Table 4.

v12 bin, mph	# samples	SSR(Xp^2|Xp)	Num. df	SSE(Xp^2,Xp)	Den. df	Test statistic	F critical	p-value	Result
-10 to 0	25	107.437	1	98.412	22	24.018	4.301	0.000	Reject H_0
0 to 10	29	121.802	1	31.811	26	99.554	4.225	0.000	Reject H_0
10 to 20	22	123.842	1	31.797	19	74.001	4.381	0.000	Reject H_0
20 to 30	17	79.705	1	77.893	14	14.326	4.600	0.002	Reject H_0
30 to 40	10	67.598	1	40.859	7	11.581	5.591	0.011	Reject H_0
40 to 50	4	23.574	1	0.029	1	810.776	161.448	0.022	Reject H_0

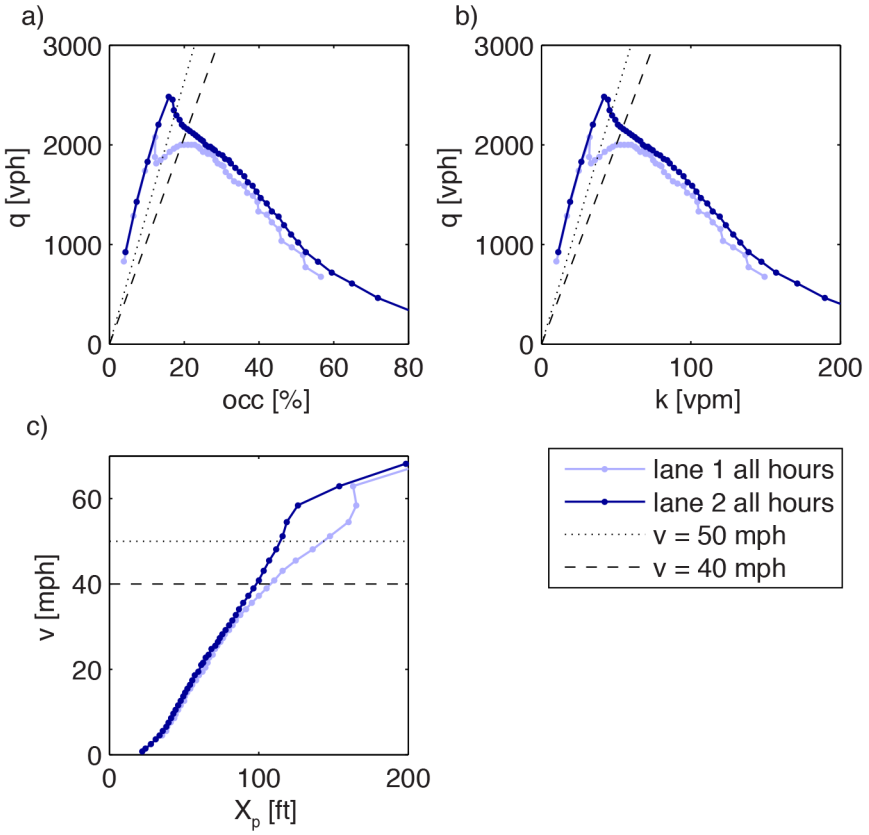

Figure 1, The empirically observed fundamental relationship from all 24 hrs of the day over 69 days, and 5 stations for 18-22 ft vehicles for the time-of-day HOV lane 1 and GP lane 2 in (a) the flow occupancy plane, (b) the flow density plane, and (c) the speed spacing plane. Note that throughout the congested regime lane 1 exhibits lower flow or higher spacing, X_p, compared to lane 2 for a given v_1.

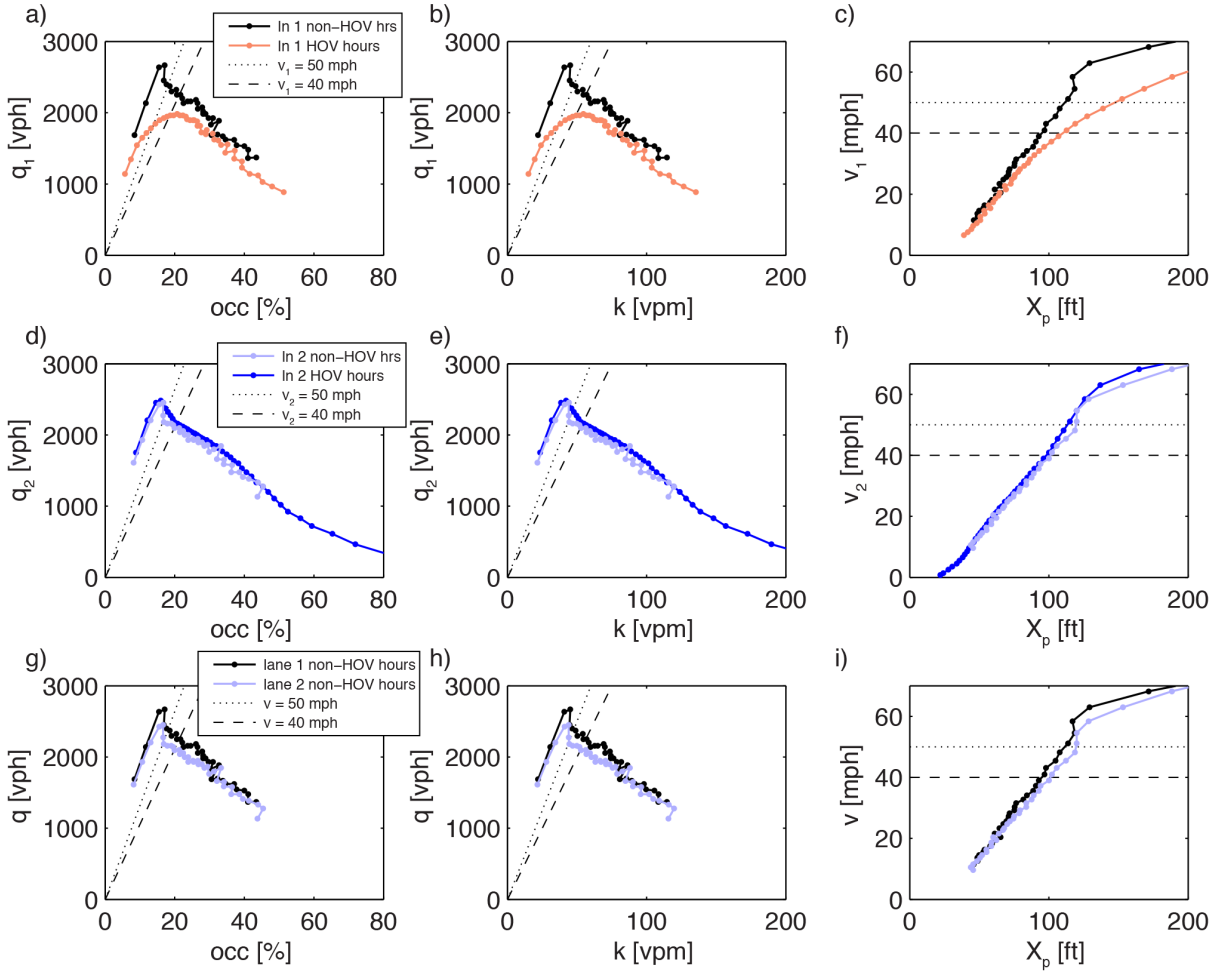

Figure 2, Repeating the plots from Fig. 1 only now sorting the data by different conditions: (a-c) the fundamental relationship in lane 1 during the HOV and non-HOV periods; (d-f) the fundamental relationship in lane 2 during the HOV and non-HOV periods; (g-i) the fundamental relationship in both lanes during the non-HOV period. It is evident that Lane 1 only exhibits a lower flow or higher spacing, X_p, during the HOV period.

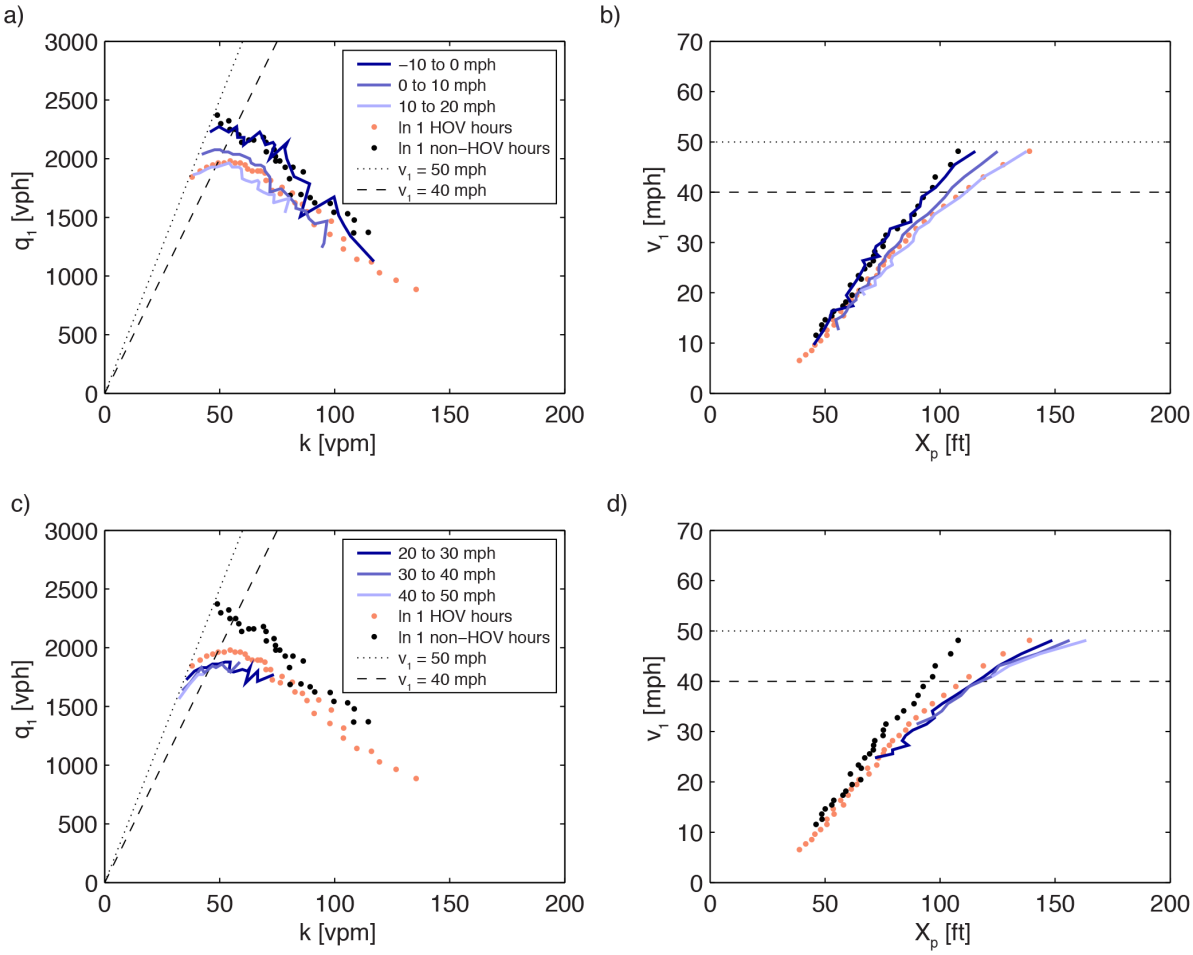

Figure 3, Repeating the HOV period data from Fig. 2b-c only now sorting by Δv_{12} bins. For reference the original curves from Fig. 2b-c are shown with points. As Δv_{12} increases the flow drops and spacing, X_p, increases for a given v_1.

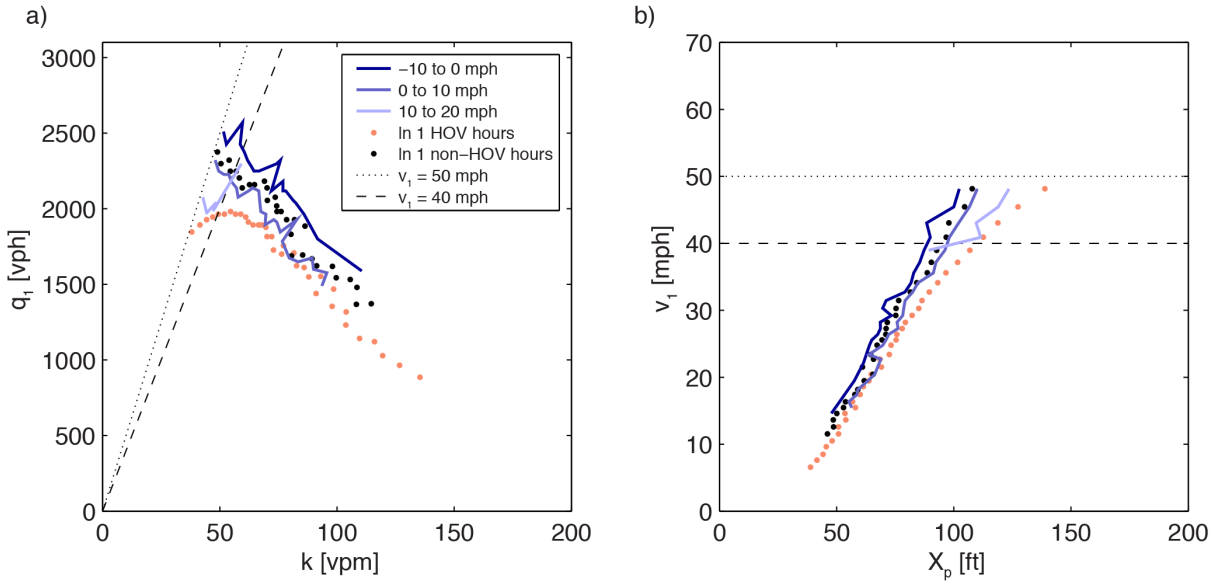

Figure 4, Repeating the non-HOV period data from Fig. 2b-c only now sorting by Δv_{12} bins. For reference the original curves from Fig. 2b-c are shown with points. Like Fig. 3, as relative speed increases the flow drops and spacing, X_p, increases for a given v_1.

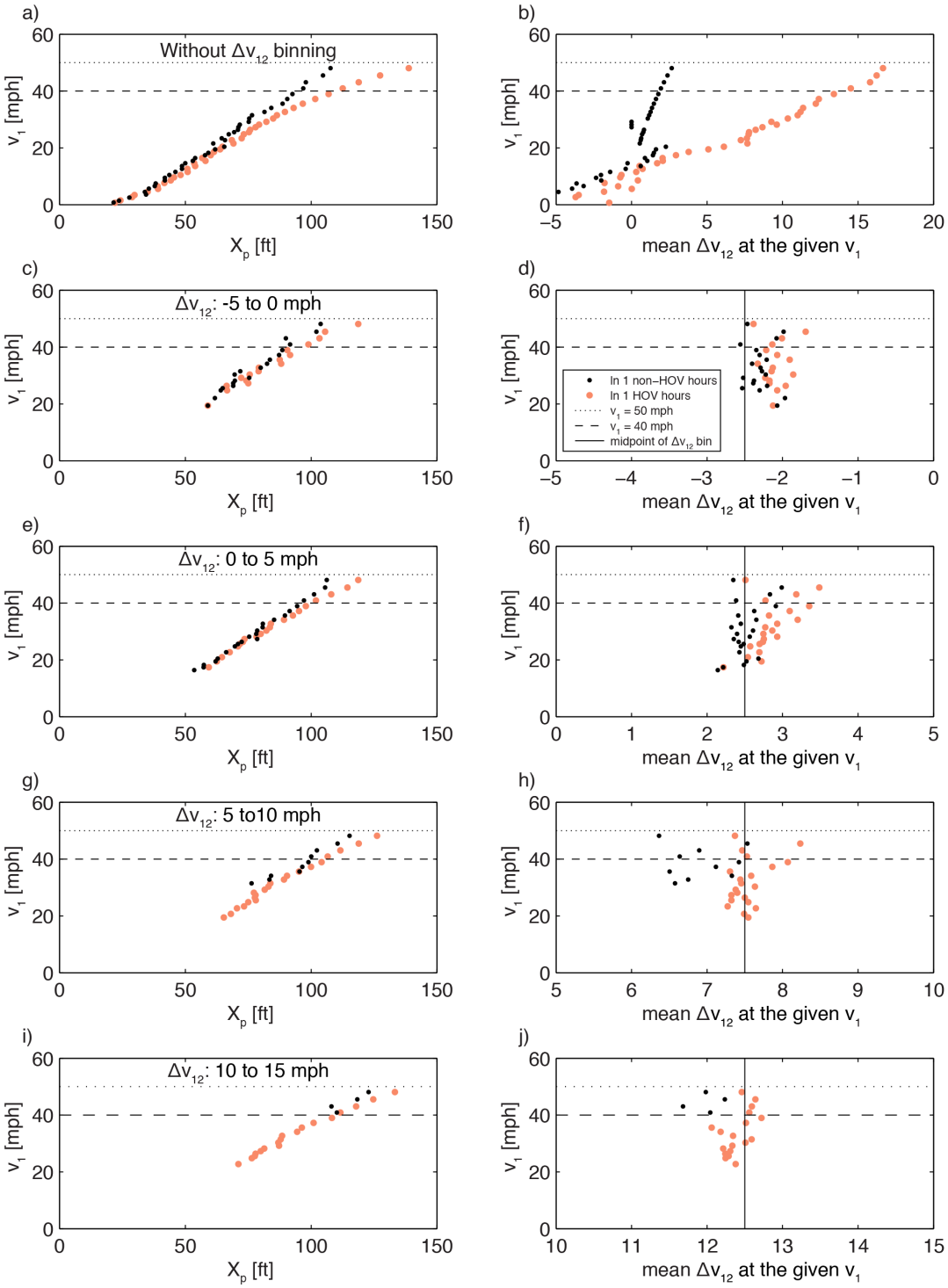

Figure 5, The left hand column of plots compare the HOV and non-HOV VXp relationships for the indicated Δv_{12} bin (similar Fig. 3b and 4b; however, the earlier figures used 10 mph Δv_{12} bins while this figure uses 5 mph Δv_{12} bins). Generally the HOV period exhibits larger spacing, X_p, than the non-HOV period for a given v_1. The right hand column of plots show the mean relative speed observed at each v_1 for the data in the VXp plot immediately to the left (note that the independent variable is plotted on the ordinate to facilitate comparison with the VXp plot). Compared to the non-HOV period, it is evident that the HOV period tends to come from higher Δv_{12} within the range of the Δv_{12} bin.

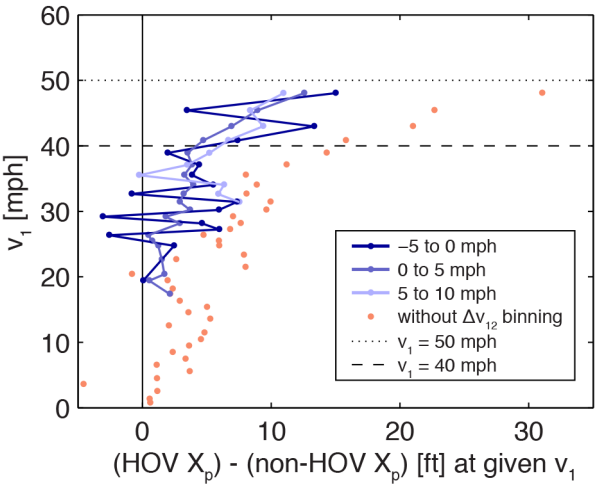

Figure 6, The difference in spacing for a given v_1 between the HOV and non-HOV periods from Fig. 5a, c, e, and g.

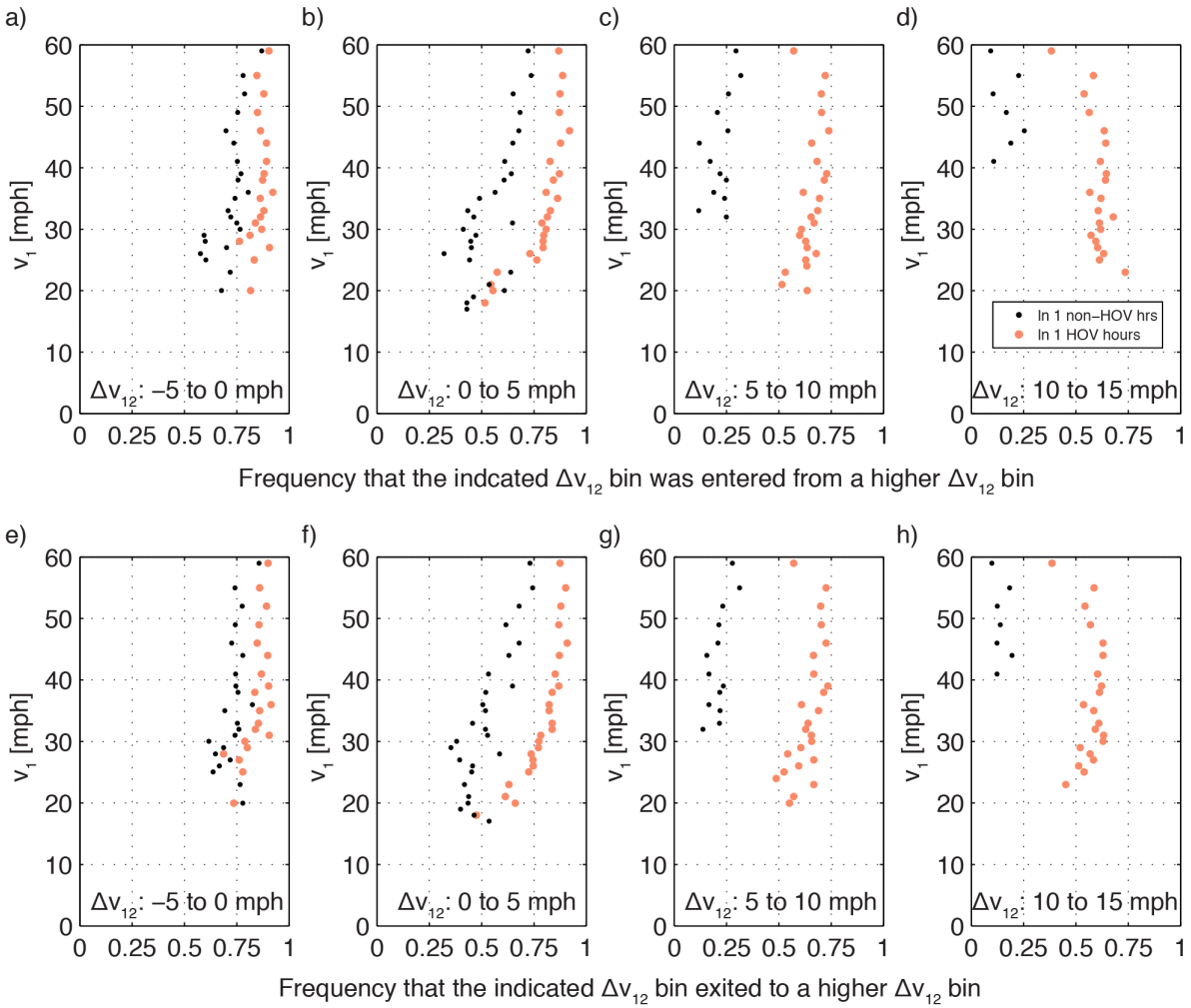

Figure 7, Reviewing the data from Fig. 5, (a-d) The proportion of times that the traffic state enters the indicated Δv_{12} bin from a higher Δv_{12} bin for the HOV and non-HOV periods (with the rest entering from a lower bin), (e-h) repeating the tallies for when the traffic state leaves a given Δv_{12} bin. Generally the HOV period enters/leaves the given bin more frequently from/to a higher Δv_{12} bin compared to the non-HOV period for a same v_1 and Δv_{12}.

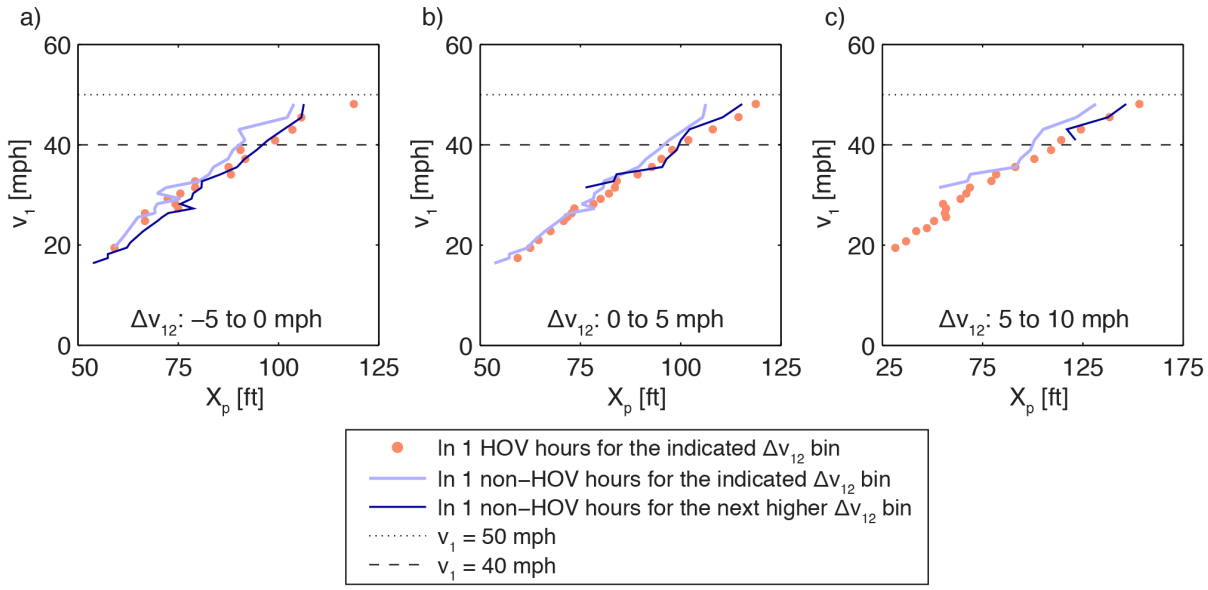

Figure 8, Repeating the comparisons of Fig. 5c, e and g for the indicated Δv_{12} bin. Now the HOV period VXp curve is shown with points and the non-HOV period VXp with the lighter shaded curve. The non-HOV VXp curve from the next higher Δv_{12} bin is shown with a darker shaded curve and generally falls closer to the HOV VXp curve for the indicated Δv_{12} bin.

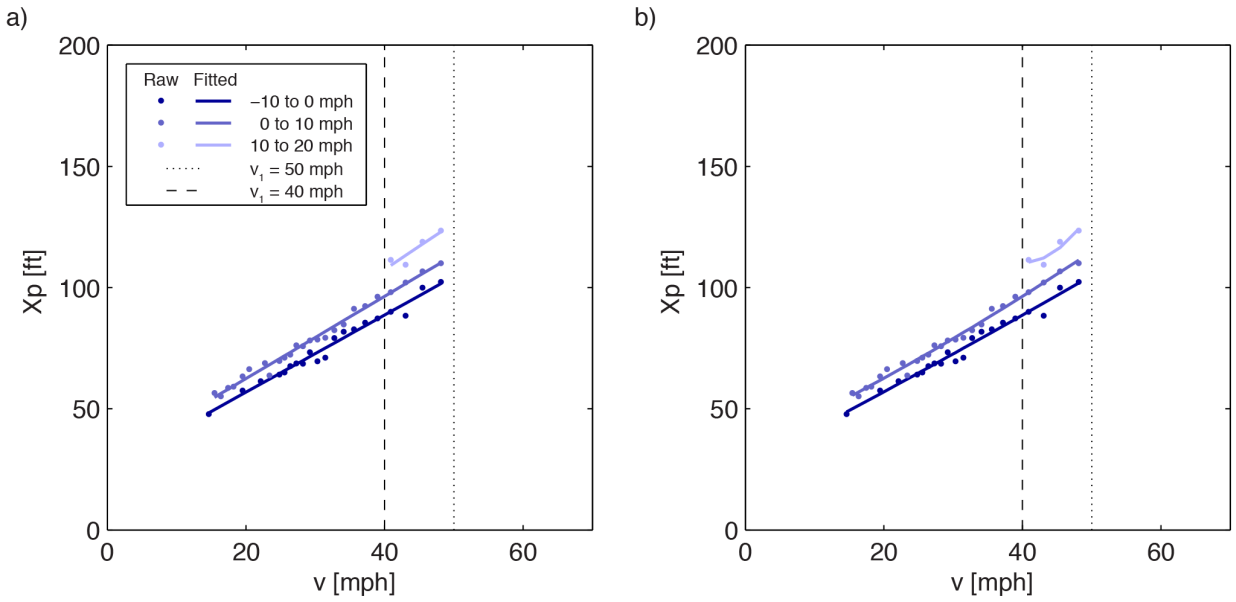

Figure 9, Linear and parabolic models for the three Δv_{12} bins during the non-HOV period, (a) linear fitted curves (b) parabolic fitted curves.

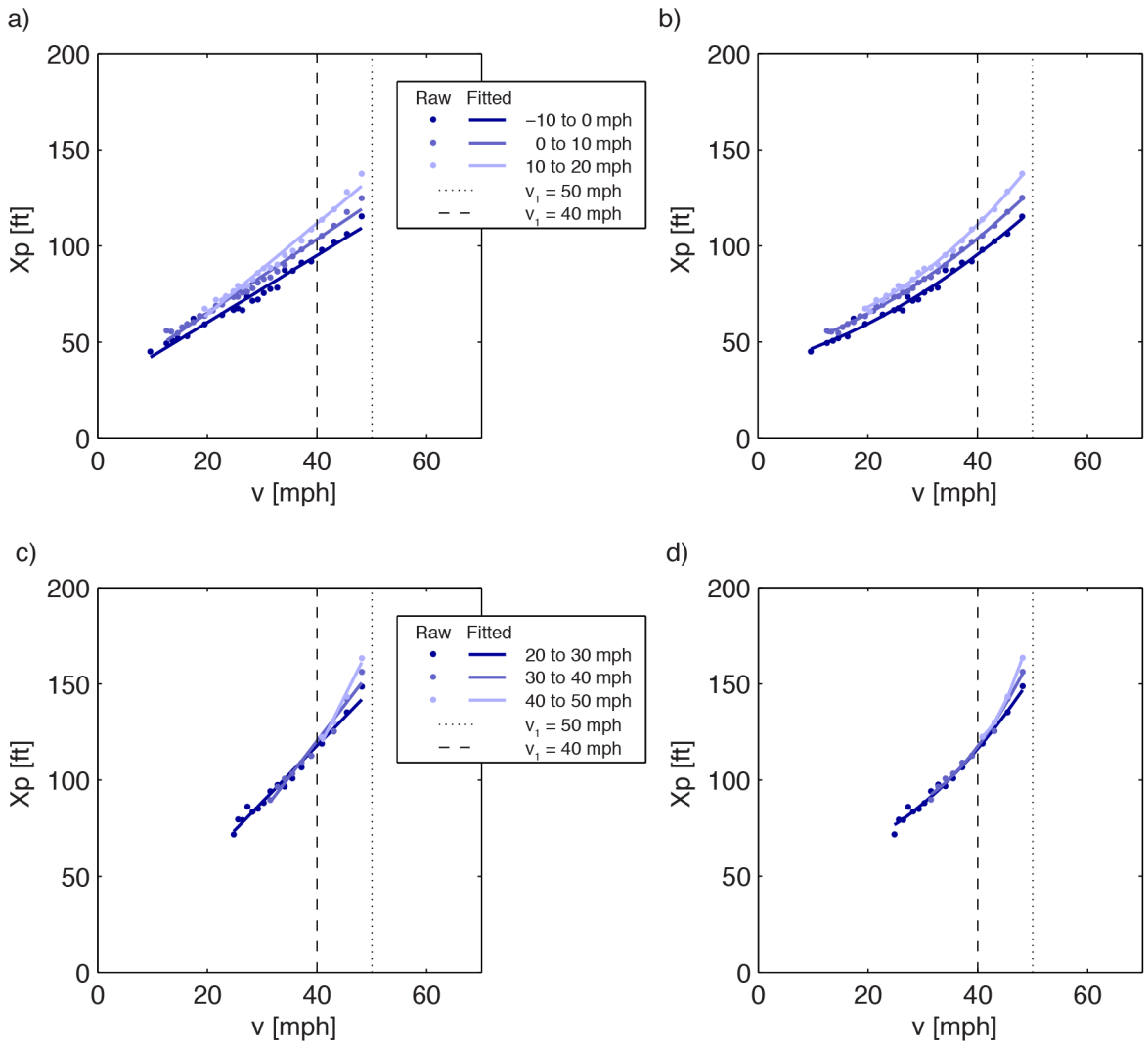

Figure 10, Linear and parabolic models for the six Δv_{12} bins during the HOV period. Top row of plots -10 to 20 mph, bottom row of plots 20 to 50 mph; left column of plots linear fitted curves, right column of plots parabolic fitted curves.